

CORRELATIONS BETWEEN RESULTS FROM COMPRESSIVE, FLEXURAL, AND TENSILE TESTS OF STEEL FIBER REINFORCED CONCRETE

Waleed Tameemi ¹, Angel L. Perez-Irizarry ², Vasily Dudnik ³, Rémy D. Lequesne ⁴, and Gustavo J. Parra-Montesinos ⁵

¹ Instructor, Babylon University, wal2005wal@yahoo.com.

² Graduate Student Researcher, University of Wisconsin-Madison, perezirizar@wisc.edu.

³ Engineer, Mid-States Concrete Industries, v.dudnik@msprecast.com.

⁴ Assistant Professor, University of Kansas, rlequesne@ku.edu.

⁵ C.K. Wang Professor, University of Wisconsin-Madison, gustavo.parra@wisc.edu.

ABSTRACT

Results are reported from a study aimed at investigating the correlation between the post-peak compressive response and the post-cracking behavior in tension and bending of various steel fiber reinforced concretes (FRC). The test program consisted of compressive, flexural, and tensile tests conducted on specimens from 24 batches of concrete. Four different types of hooked-end steel fibers were used in volume fractions of 0.5, 0.75, 1.0, and 1.5%. Concrete mixtures had a target compressive strength of either 41 or 69 MPa. Of the parameters investigated, it was found that the post-peak slope of FRC in compression was most correlated with the peak post-cracking flexural strength and the flexural strength measured at a mid-span deflection of approximately $L/450$ (1 mm) for an ASTM C1609-compliant specimen with a depth of 150 mm. Scatter in flexural and tensile test results decreased significantly when T_{50} , a relative measure of viscosity, was greater than one second.

Keywords: FRC, compression, tension, flexure, post-cracking behavior, steel hooked fibers, stress-strain response

Rémy D. Lequesne, PhD, P.E.
University of Kansas
1530 W. 15th St., Rm. 2150 Learned Hall
Lawrence, Kansas 66045
United States

Email: rlequesne@ku.edu
Tel: 785-864-6849

1. INTRODUCTION

Well distributed, discreet deformed steel fibers provide resistance to opening and propagation of cracks in concrete. As a result, use of fiber reinforced concrete (FRC) usually leads to improved shear strength and deformation capacity in reinforced concrete members [1, 2].

Despite the advantages of using FRC, there are also challenges that have slowed the widespread adoption of FRC materials in practice [3]. One of these challenges is the difficulty of conducting the multiple quality control tests required to characterize the load-deformation response of an FRC mixture. In particular, engineers may be unable to use the post-peak compression response of FRC, which can be similar to that of well confined concrete, in design without a consistent and readily available means of specifying and verifying performance.

To potentially limit the scope of the test program required to characterize FRC behavior, the current study examines correlations between the post-peak response of FRC under compression and post-cracking results from flexural and tensile tests. Results may lead to indirect means of qualifying FRC mixtures for use in applications that benefit from the post-peak toughness of FRC.

2. RESEARCH SIGNIFICANCE

Results from tensile, compressive, and flexural tests are reported for FRC mixtures having four different types of fibers in volume fractions of 0.5, 0.75, 1.0, and 1.5%. An effort has been made to quantify the extent to which the results from different types of tests are correlated, with the aim of reducing the number of types of tests required to characterize and qualify FRC mixtures for use in practice. Reported results indicate that mixtures with T_{50} values less than one second are prone to exhibit a high amount of scatter in tests of mechanical properties.

3. MATERIALS

3.1. Concrete Mixtures

Self-consolidating concrete was used as the base for the FRC used in this study to eliminate potential workability problems associated with addition of large amounts of fibers. The result, which has been called self-consolidating fiber reinforced concrete, is a highly workable concrete after addition of fibers [4]. No vibration or rodding was therefore used when casting the specimens.

Concrete mixtures with target compressive strengths of 41 and 69 MPa were used in this study. The mixture proportions prior to addition of fibers are listed in Table 1.

Table 1. Concrete proportions per cubic meter

Constituent Material	Target Compressive Strength	
	41 MPa	69 MPa
Type I Portland Cement (kg)	372	601
Class C Fly Ash (kg)	326	150
Kansas River Sand (kg)	818	852
Kansas River Rock ^a (kg)	446	501
Water (kg)	286	218
VMAR 3 (mL)	6250	3530
ADVA 195 (mL)	544	4320

^a 10 mm maximum aggregate size

3.2. Fiber Types

The four types of hooked-end steel fibers used in this study are shown in Figure 1. These are the RC-80/30-BP fiber, with a length of 30 mm, an aspect ratio of 80, and a tensile strength of 2300 MPa; the RC-55/30-BG fiber, with a length of 30 mm, an aspect ratio of 55, and a tensile strength of 1350 MPa; the 4D RC-65/60-BG fiber, with a length of 60 mm, an aspect ratio of 65, and a tensile strength of 1500 MPa; and the 5D RC-65/60-BG fiber, with a length of 60 mm, an aspect ratio of 65, and a tensile strength of 2300 MPa. All four fibers are manufactured by Bekaert Corporation.

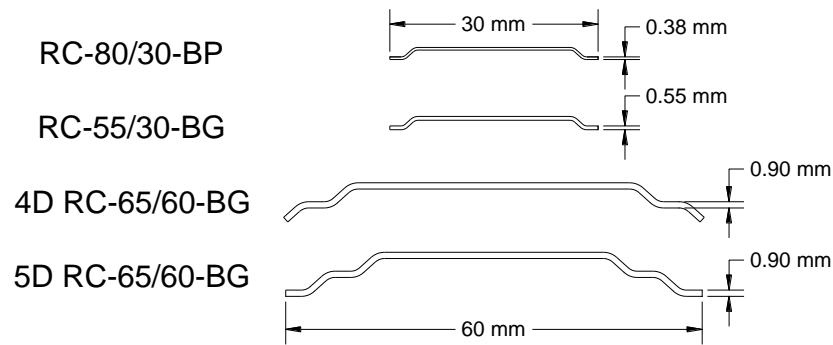


Figure 1. Fiber types

4. TEST PROGRAM

A series of tests were conducted on FRC mixtures having a target compressive strength of either 41 or 69 MPa. Except for two batches that did not have fibers, each batch of concrete had one of four types of hooked steel fibers in volume fractions of 0.5, 0.75, 1.0, or 1.5%. Table 2 shows all combinations of fiber type and volume fraction that were considered in this study. Specimens from each batch were subjected to a test program consisting of compressive, flexural (un-notched beams), and tensile tests conducted on five samples of each type.

Table 2. Summary of concrete mixtures, fiber types and fiber volume fractions used in this study

Target Compressive Strength	Fiber Type	Fiber Volume Fraction (%)				
		0	0.5	0.75	1.0	1.5
41 MPa	No Fibers	a				
	RC-80/30-BP		a	a	a	a
	RC-55/30-BG		a	a	a	a
	4D RC-65/60-BG		a	a	a	a
	5D RC-65/60-BG			a		a
69 MPa	No Fibers	a				
	RC-80/30-BP		a	a	a	a
	4D RC-65/60-BG			a		a
	5D RC-65/60-BG			a		a

^a For each mixture, a single batch was used to fabricate five cylinders for compression tests, five un-notched beams for flexural tests, and five notched prisms for uniaxial tension tests.

4.1. Uniaxial Compression Tests

Compression tests were conducted on 150 by 300 mm cylindrical concrete specimens in accordance with ASTM C39 [5] using a 2670 kN hydraulic test frame. An infrared-based non-contact position sensor system was used to record the position of 16 independent markers fixed to the specimen and test frame (shown in Figure 2). Up to the peak load, longitudinal strains were calculated based on the displacement of markers numbered 3, 4, 7, and 8. After the peak load, the relative displacement between

loading platens (recorded with markers numbered 15 and 16) was used to estimate longitudinal cylinder strains because the location of markers fixed to the specimen became sensitive to localized damage.

The feature of the test results most relevant to the current study was the post-peak slope of the recorded stress versus longitudinal strain curve. The post-peak slope was defined as the slope of a line from the peak of the stress versus strain curve to a point representing a 50% loss of strength. This slope was then divided by the peak compressive strength of the specimen to obtain a unitless measure of post-peak slope, Z . This definition of Z has been applied previously to confined concrete [6].

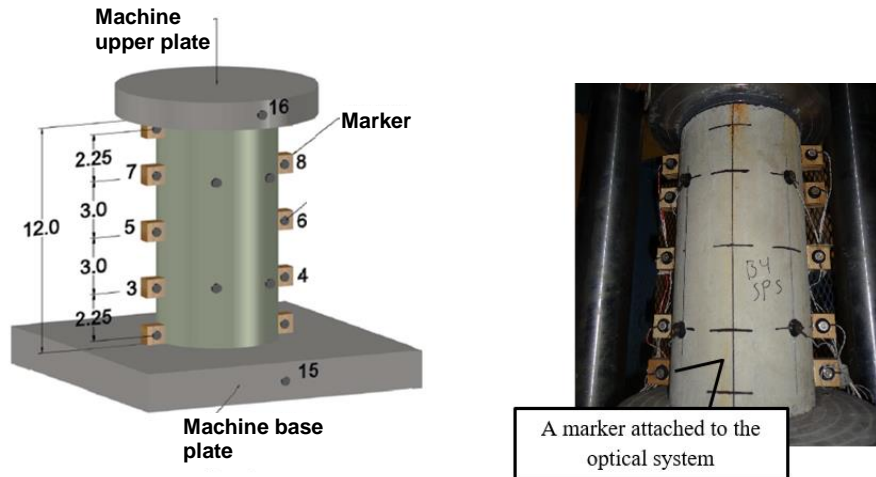


Figure 2. Typical compression test specimen and location of instrumentation (1 in. = 25 mm)

4.2. Flexural Tests

Un-notched beams with dimensions of 150 by 150 by 510 mm were tested under four-point bending in general accordance with ASTM C1609 [7]. One important change from the standard procedure was that an infrared-based non-contact position sensor system was used instead of LVDTs to record beam deflections. The position sensor system recorded the displacement of 16 markers attached to one side of each specimen in the arrangement shown in Figure 3. Mid-span deflection was calculated using the displacement of markers 1, 5, 6, and 9. Although not reported herein, the displacement data were also used to calculate beam rotations at several sections and to estimate the width of the dominant crack at the bottom face of the beam. More detailed results are reported in Reference [8].

4.3. Direct Tensile Tests

The relationship between tensile stress and crack width was evaluated using a tension test proposed in Reference [9]. The specimens consist of a 150 by 150 by 510 mm concrete prism cast with a 16 mm diameter reinforcing bar oriented along its centroidal longitudinal axis. The reinforcing bar is discontinuous at the center of the specimen, where a 19 mm deep notch is cut around the perimeter of the prism (Figure 4). Under load, a crack forms at the notched section. The width of the crack was calculated using the recorded location of eight markers placed along the edges of the notch, accounting for any rotation (reported crack widths represent an average width).

4.4. Tests of Fresh-State Properties

The fresh-state properties of each batch were documented using standard test methods (complete results are presented in Reference [8]). Of most interest to this study were the results from tests for slump flow and T_{50} performed in accordance with ASTM C1611 [10]. The T_{50} test is a non-mandatory and indirect means of evaluating the viscosity of self-consolidating concrete. T_{50} , measured during a slump flow test, is the time it takes after lifting of the mold for the outer edge of the spreading concrete patty to reach a diameter of 50 cm. Larger T_{50} values are correlated with higher concrete viscosity.

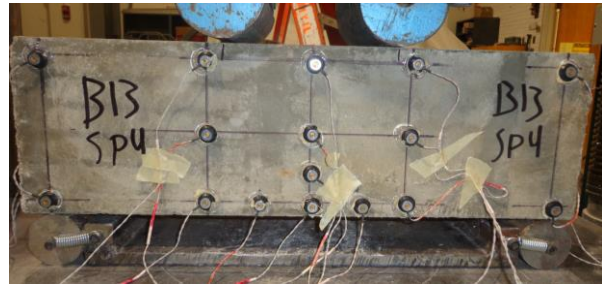
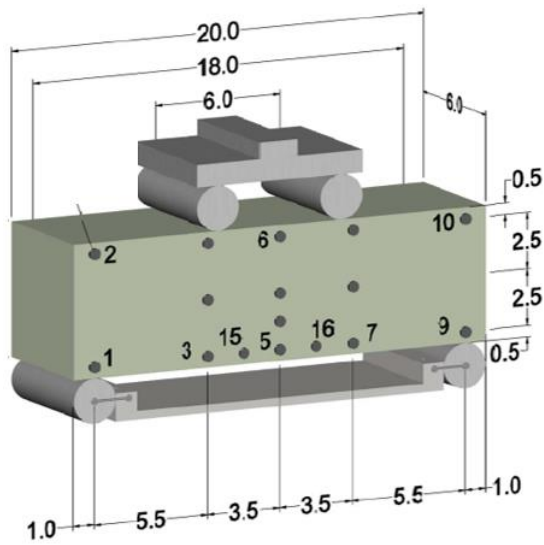
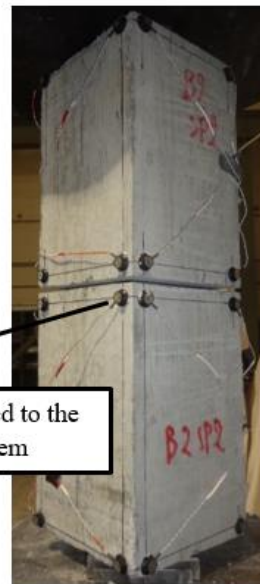
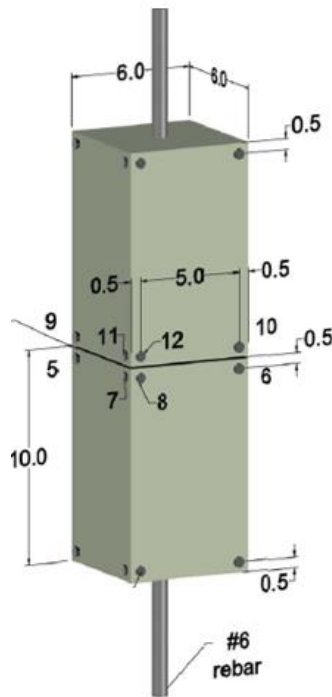


Figure 3. Typical flexural test specimen and location of instrumentation (1 in. = 25 mm)



A marker attached to the Optical system

Figure 4. Typical tension test specimen and location of instrumentation (1 in. = 25 mm)

5. RESULTS

Typical results are shown in Figure 5 from tests of cylinders in compression (Figure 5a), un-notched beams in bending (Figure 5b), and notched prisms under tension (Figure 5c) for one of the fibers evaluated (RC-80/30-BP). Each of the curves in Figure 5 is the result of a single test selected from the data recorded for mixtures having either no fibers or RC-80/30-BP fibers in a volume fraction of either 0.5 or 1.5%. As described below, the effects that use of fibers have on the post-peak response in compression and the post-cracking response in bending and tension are evident in Figure 5.

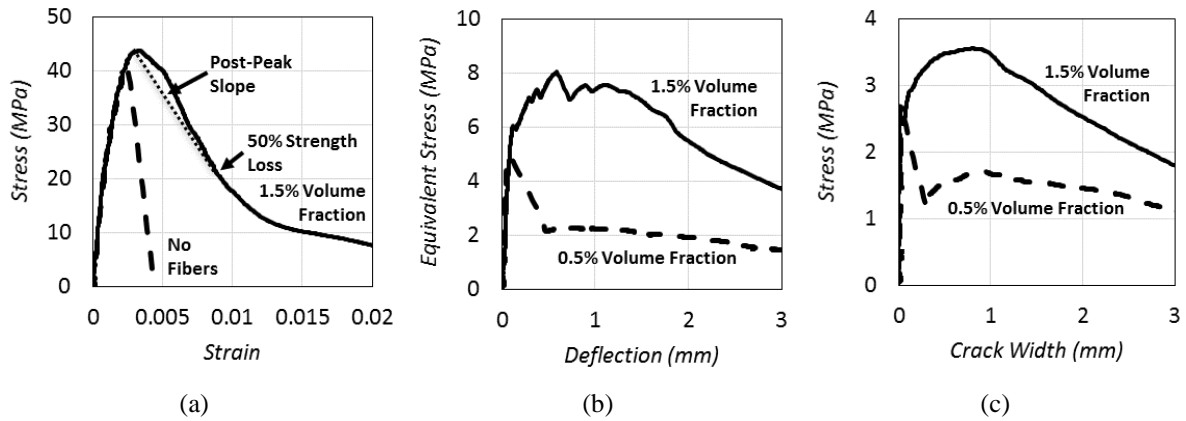


Figure 5. Typical results from (a) compressive, (b) flexural, and (c) tensile tests of specimens with RC-80/30-BP fibers

5.1. Compressive Test Results

The fibers used in this study had a negligible effect on concrete compression strength and initial modulus (Figure 5a). However, the compression toughness, calculated as the area under the compression stress versus longitudinal strain curve, increased as fiber amount increased.

The post-peak slope in compression, approximated as the slope of a line drawn from the peak stress to a point representing a 50% loss of strength (Figure 5a), was significantly affected by both fiber type and fiber volume fraction. The post-peak slope is represented herein as Z , which is defined as the slope divided by the peak compressive strength. Values of Z are listed in Table 3 and plotted versus fiber volume fraction in Figure 6.

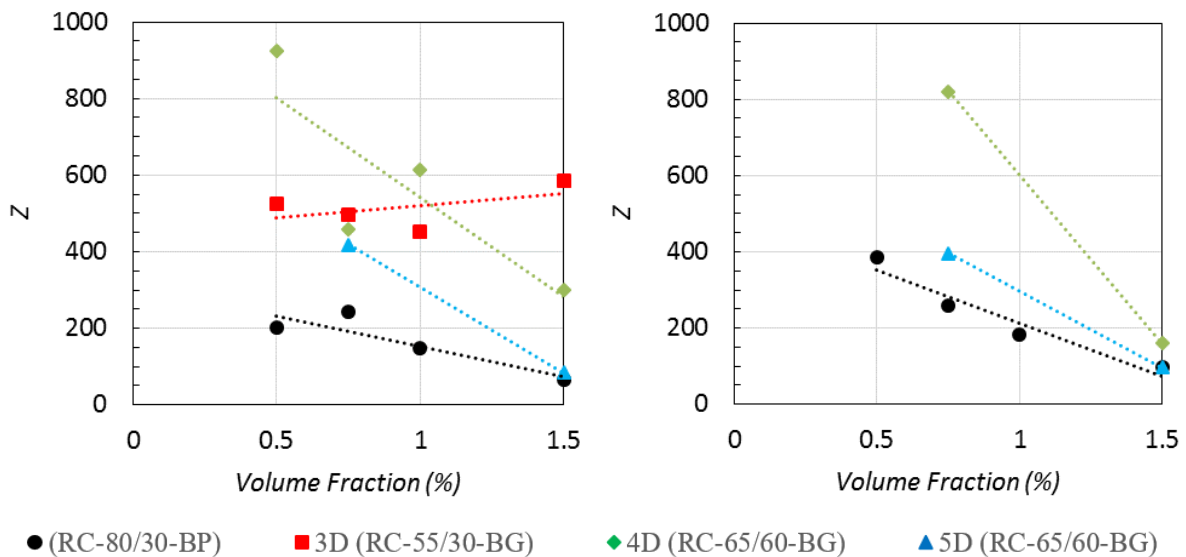


Figure 6. Normalized post-peak slope, Z , versus fiber volume fraction (target compressive strength of 41 and 69 MPa, left and right, respectively)

Each point in the Figure 6 plots represents an average value for specimens tested for each batch. As shown in Figure 6, Z became closer to zero as fiber volume fraction increased. At a volume fraction of 1.5%, most batches exhibited average Z values less than 300, with some as low as 70. At lower volume fractions, calculated values of Z were more sensitive to fiber type. Batches with a 0.5% volume fraction of RC-80/30-BP fibers exhibited average Z values less than 400, whereas the batch with a 0.5% volume fraction of 4D RC-65/60-BG fibers and a target compressive strength of 41 MPa had a calculated Z value of approximately 800.

Although overall Figure 6 also shows a modest trend between Z and fiber type, scatter in results limits the significance of observed differences. Specimens with fiber type RC-80/30-BP, with an aspect ratio of 80, tended to perform better than other specimens for all volume fractions.

5.2. Flexural Test Results

The peak post-cracking equivalent flexural stress (σ_{fp}), divided by the stress on the bottom of the section at first cracking (σ_{fc}), is shown in Table 3. Both σ_{fp} and σ_{fc} were calculated with Eq. 1:

$$\sigma_f = \frac{PL}{bh^2} \quad (1)$$

where: P is the force applied to the specimen, L is the clear span length, and b and h are the width and height of the specimen at the location of the governing crack. Note that σ_{fp} is an equivalent stress calculated assuming a linear distribution of stress about mid-depth. Batches with σ_{fp}/σ_{fc} greater than 1.0 exhibited, on average, greater strength after first cracking, referred to as deflection hardening behavior. The response plotted in Figure 5b for the mixture with a fiber volume fraction of 1.5% is an example of deflection hardening behavior.

For a target compressive strength of 41 MPa, specimens with the RC-80/30-BP fiber in volume fractions of 0.75% and greater exhibited deflection hardening behavior. For batches with both the 4D RC-65/60-BG and 5D RC-65/60-BG fibers, a volume fraction of 1.5% was necessary for specimens to, on average, exhibit deflection hardening behavior. Deflection hardening behavior was not exhibited by any specimens with RC-55/30-BG fibers.

Table 3. Summary of results from compressive, flexural and tensile tests on FRC

Target Compressive Strength	Fiber Type	V_f (%)	Z	$\sigma_{fp} / \sigma_{fc}$	$\sigma_{tp} / \sigma_{tc}$
41 MPa	N/A	0	1080	-	-
	RC-80/30-BP	0.5	200	0.87	0.55
	RC-80/30-BP	0.75	241	1.01	0.98
	RC-80/30-BP	1.0	148	1.26	1.05
	RC-80/30-BP	1.5	66.0	1.15	1.32
	RC-55/30-BG	0.5	526	0.21	0.13
	RC-55/30-BG	0.75	497	0.45	0.31
	RC-55/30-BG	1.0	453	0.59	0.51
	RC-55/30-BG	1.5	585	0.74	0.61
	4D RC-65/60-BG	0.5	924	0.47	0.73
	4D RC-65/60-BG	0.75	458	0.78	0.90
	4D RC-65/60-BG	1.0	615	0.95	1.04
	4D RC-65/60-BG	1.5	299	1.21	1.37
	5D RC-65/60-BG	0.75	418	0.84	0.67
	5D RC-65/60-BG	1.5	83.6	1.29	1.16
69 MPa	N/A	0	1540	-	-
	RC-80/30-BP	0.5	386	0.91	0.66
	RC-80/30-BP	0.75	260	1.09	0.72
	RC-80/30-BP	1.0	184	1.59	1.08
	RC-80/30-BP	1.5	95.9	1.49	1.16
	4D RC-65/60-BG	0.75	821	1.00	0.79
	4D RC-65/60-BG	1.5	160	1.33	1.04
	5D RC-65/60-BG	0.75	396	1.12	0.93
	5D RC-65/60-BG	1.5	96.3	1.32	1.18

Values of σ_{fp}/σ_{fc} tended to increase for all fiber types and volume fractions for batches with a target compressive strength of 69 MPa relative to batches with a target compressive strength of 41 MPa. Although the minimum volume fraction required to cause deflection hardening behavior for batches with the RC-80/30-BP fiber remained 0.75%, the post-cracking strength increased by approximately 25% for volume fractions of 1 and 1.5%. The post-cracking behavior of specimens with both the 4D RC-65/60-BG and 5D RC-65/60-BG fibers also improved, as a volume fraction of 0.75% was sufficient to, on average, result in deflection hardening behavior. This would be consistent with concrete breakout having an important role in the behavior of specimens with lower strength concrete.

5.3. Tensile Test Results

Similar to the flexural test results, the ratio of peak post-cracking tensile strength (σ_{tp}) to first cracking tensile strength (σ_{tc}) was used as a measure of specimen performance (Table 3). Specimens with a σ_{tp}/σ_{tc} value greater than 1.0, which indicates the FRC had greater tensile strength after cracking than at cracking, are said to exhibit strain-hardening behavior (illustrated in Figure 5c). This σ_{tp}/σ_{tc} ratio was sensitive to both fiber type and fiber volume fraction.

For target compressive strengths of 41 and 69 MPa, all batches with fiber volume fractions of 1.0 and 1.5% exhibited tensile strain hardening behavior, except for those with fiber type RC-55/30-BG. No batch with the RC-55/30-BG fibers exhibited strain hardening behavior. Comparing batches with a target compressive strength of 41 and 69 MPa, there is a slight trend towards smaller σ_{tp}/σ_{tc} values as concrete compressive strength increased. This trend is different from that observed in the flexural tests, which generally showed increased σ_{fp}/σ_{fc} values with increased concrete compressive strength.

6. CORRELATIONS BETWEEN TEST RESULTS

An aim of this study was to determine the extent to which the behavior exhibited by FRC in tests of mechanical behavior are correlated. Of particular interest was the correlation between the post-peak slope of FRC tested in compression and the post-cracking results from flexural and tensile tests.

The analyses conducted do not explicitly consider differences between batches due to fiber type and volume fraction. Rather, if a high degree of correlation is observed between results from compressive, flexural, and tensile tests, it will be interpreted as an indication that differences in behavior resulting from fiber type and volume fraction are implicitly included.

For these analyses, the degree to which two parameters are correlated was quantified using the Pearson product-moment correlation coefficient, r . Values of r range from -1.0 to 1.0, where -1.0 indicates a perfect negative correlation, 0.0 indicates no correlation, and 1.0 indicates a perfect positive correlation. No definite threshold was selected to indicate a high degree of correlation. Instead, calculated r values were interpreted as being relative, with r values closer to 1.0 indicative of higher correlation.

6.1. Correlations between Compressive and Flexural Test Results

Calculated values of Z were compared to several parameters derived from the flexural tests, including the peak equivalent stress exhibited by the specimen after cracking and the equivalent stress resisted by the beam at deflections of $L/450$, $L/300$, and $L/150$ (1, 2, and 3 mm).

It was observed that Z was most closely correlated with the maximum equivalent stress exhibited by the specimen after cracking (σ_{fp}) and the equivalent stress resisted by the beam at a mid-span deflection of $L/450$ ($\sigma_{\delta = L/450}$). These trends are plotted in Figure 7 as equivalent stress resisted by the flexural specimen versus Z , where the coordinates for each point represent average values for all specimens tested for each batch. The r values calculated for σ_{fp} versus Z were -0.72 and -0.74 for the 41 and 69 MPa mixtures, respectively. For $\sigma_{\delta = L/450}$ versus Z , calculated r values were -0.70 and -0.66 for the 41 and 69 MPa mixtures.

Two observations can be made. The calculated r values are relatively high given the scatter in the results for both σ_{fp} and $\sigma_{\delta = L/450}$, indicating that, independent of the type and amount of hooked steel fiber used,

compression and flexural test results are correlated. It is also clear that compressive strength has an important influence on the relationship.

6.2. Correlations between Compressive and Tensile Test Results

The peak post-cracking tensile stress (σ_{tp}) and the tensile stress at a crack width of 1.3 mm ($\sigma_{\omega = 1.3 \text{ mm}}$) are the tensile test parameters most closely correlated to Z . Figure 8 shows plots of σ_{tp} and $\sigma_{\omega = 1.3 \text{ mm}}$ versus Z , where the coordinates for each point represent average values for all specimens tested for each batch. The r values calculated for σ_{tp} versus Z were -0.47 and -0.62 for the 41 and 69 MPa mixtures. For $\sigma_{\omega = 1.3 \text{ mm}}$ versus Z , calculated r values were -0.46 and -0.62 for the 41 and 69 MPa mixtures.

Although the calculated r values indicate a negative correlation, these tensile test parameters are not as closely correlated to Z as the flexural test parameters plotted in Figure 7. Similar to Figure 7, Figure 8 shows that concrete compressive strength has an important influence on the relationships.

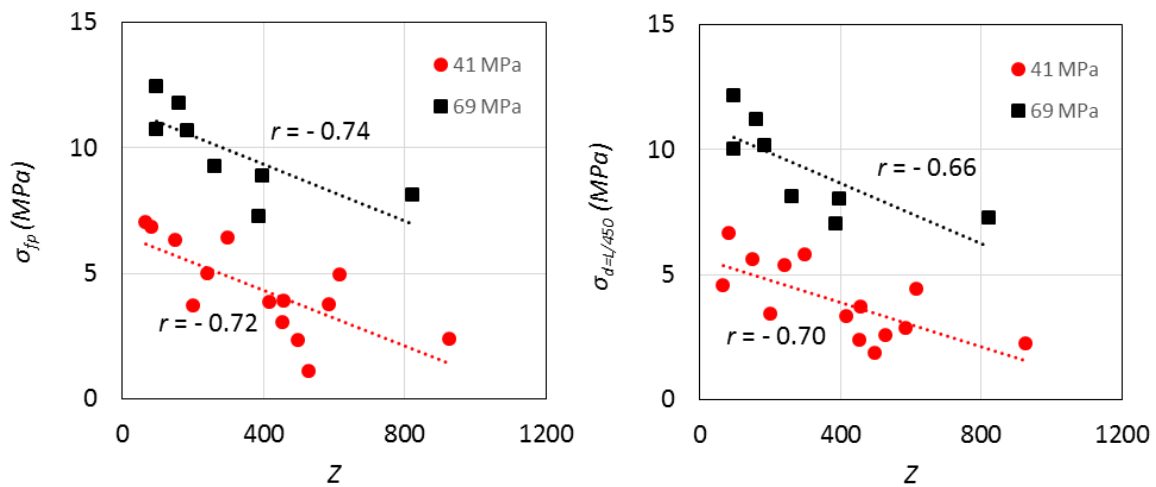


Figure 7. Equivalent stress resisted by beam specimens at peak post-cracking strength and at a deflection of $L/450$ (left and right, respectively) plotted versus Z

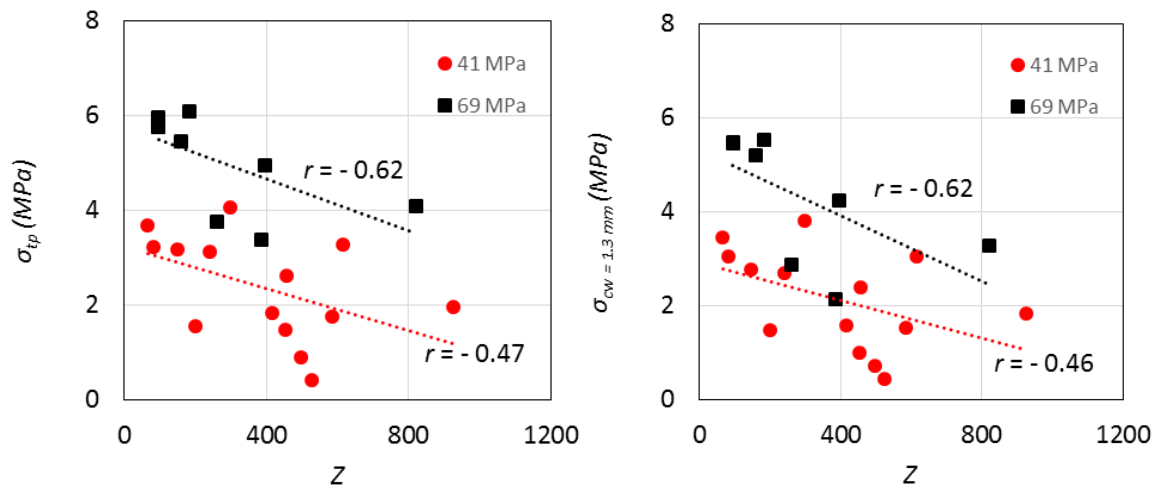


Figure 8. Average tensile stress at peak post-cracking strength and at a crack width of 1.3 mm (left and right, respectively) plotted versus Z

6.3. Correlations between Within-Batch Scatter (COV) and T_{50} Results

Figure 9 shows the coefficient of variation (COV) calculated for the peak post-cracking strength recorded from flexural and tensile tests plotted versus T_{50} . Both COV and T_{50} correspond to individual batches of concrete. It is clear that specimens from batches with T_{50} values less than 1 second exhibited higher scatter in post-cracking behavior (in terms of within-batch COV). This was more evident for the peak post-cracking stress observed in flexural tests: for batches with T_{50} values less than 1.0 second, the average COV calculated for the peak post-cracking loads was 40%, whereas batches with a T_{50} value of at least 1.0 second had an average COV of 13%. There was no correlation between T_{50} values and the variation of the post-peak slope in compression.

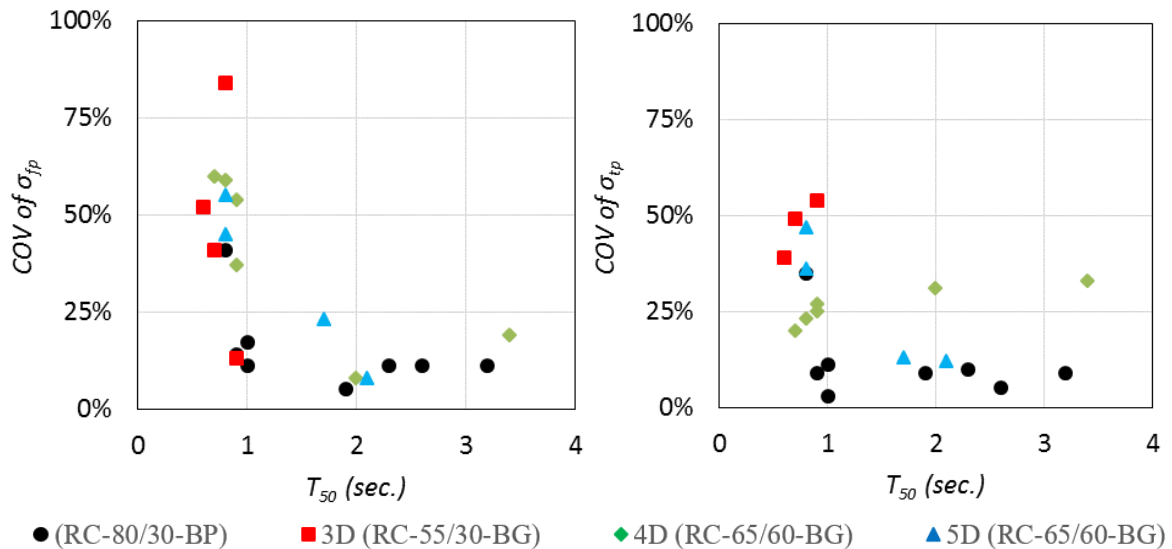


Figure 9. Coefficient of variation calculated for the peak post-cracking load in bending (P_{fp}) and the peak post-cracking stress in tension (σ_{tp}), plotted versus T_{50}

7. SUMMARY AND CONCLUSIONS

Results are reported from an experimental study aimed at investigating the correlation between results from flexural, tensile, and compressive tests of various fiber reinforced concrete (FRC) materials. Four different types of hooked-end steel fibers were used in volume fractions of 0.5, 0.75, 1.0, and 1.5%. Concrete mixtures had a target compressive strength of either 41 or 69 MPa. Findings include:

- The post-peak slope of FRC in compression (represented as Z) was more closely correlated to results from un-notched flexural tests (tested per ASTM C1609) than direct tensile tests. Values of Z were most correlated with the peak post-cracking equivalent stress ($r \cong 0.73$) and the equivalent stress resisted by the beam at a deflection of $L/450$ ($r \cong 0.68$).
- The coefficient of variation calculated for the peak post-cracking strength in both tension and bending decreased significantly when T_{50} was greater than one second. This was particularly evident for results from flexural tests, which had a COV of 40% when T_{50} was less than one second and 13% when T_{50} was greater than 1 second.
- The ratio of peak post-cracking equivalent stress to the stress associated with cracking increased for all fiber types and volume fractions when the target compressive strength increased from 41 to 69 MPa. This is consistent with local concrete breakout caused by fibers having an important role in the behavior of specimens with lower strength concrete.

ACKNOWLEDGMENTS

Materials used for this study were donated by Bekaert Corporation, Midwest Concrete Materials, Inc., W.R. Grace and Company, and Gerdau Ameristeel Corporation. The opinions expressed in this article are those of the authors and do not necessarily represent the views of the sponsors.

REFERENCES

- [1] ACI Committee 544. (1996, Reapproved 2009). *544.1R-09: Report on Fiber Reinforced Concrete*. Farmington Hills, MI: American Concrete Institute.
- [2] Parra-Montesinos, G. J. (2005). High-Performance Fiber-Reinforced Cement Composites: An Alternative for Seismic Design of Structures, *ACI Structural Journal*, 102(5), 668-675.
- [3] Mindess, S. (2014). FRC in Structural Applications, *Proceedings: FRC 2014 Joint ACI-fib International Workshop: Fiber Reinforced Concrete: from Design to Structural Applications*, Montreal, Canada, July 24-25.
- [4] Liao, W.-C., Chao, S.-H., Park, S.-Y., and Naaman, A. E. (2006). *Self-Consolidating High Performance Fiber Reinforced Concrete (SCHPFRC) - Preliminary Investigation*. Ann Arbor, USA: University of Michigan.
- [5] ASTM Standard C39. (2015). *Standard Test Method for Compressive Strength of Cylindrical Concrete Specimens*, West Conshohocken, Pennsylvania, ASTM International.
- [6] Kent, D.C. and Park, R. (1971). Flexural Members with Confined Concrete, *Journal of the Structural Division*, 97(7), 1969-1990.
- [7] ASTM Standard C1609. (2012). *Standard Test Method for Flexural Performance of Fiber-Reinforced Concrete (Using Beam With Third-Point Loading)*, West Conshohocken, Pennsylvania, ASTM International.
- [8] Tameemi, W., and Lequesne, R. (2015). *SM Report No. 114: Correlations between Compressive, Flexural, and Tensile Behavior of Self-Consolidating Fiber Reinforced Concrete*. Lawrence, Kansas: University of Kansas Center for Research.
- [9] Parra-Montesinos, G. J., Wight, J. K., Kopczynski, C., Lequesne, R. D., Setkit, M., Conforti, A., and Ferzli, J. (2014). Earthquake-Resistant Fiber Reinforced Concrete Coupling Beams Without Diagonal Bars. *Proceedings: FRC 2014 Joint ACI-fib International Workshop: Fiber Reinforced Concrete: from Design to Structural Applications*, Montreal, Canada, July 24-25.
- [10] ASTM Standard C1611. (2014). *Standard Test Method for Slump Flow of Self-Consolidating Concrete*, West Conshohocken, Pennsylvania, ASTM International.